

## Energetics and electronic structures of chemically decorated C<sub>60</sub> chains

Sho Furutani\* and Susumu Okada†

*Graduate School of Pure and Applied Sciences, University of Tsukuba, Tsukuba, Ibaraki 305-8571, Japan*

---

We studied the energetics and electronic structures of one-dimensional molecular chains of [6,6]-phenyl-C<sub>61</sub>-butyric acid methyl ester (PCBM) using the density functional theory (DFT). Our DFT calculations show that the binding energies of PCBM range from 90 to 300 meV, depending on not only the intermolecular spacing but also the intermolecular arrangements owing to the interaction between functional groups and C<sub>60</sub>. The electronic structure of PCBM chains are also sensitive to the mutual arrangements of PCBM in their chain structure. The calculated effective masses of the conduction band range from 0.58 to 634.97  $m_e$ , giving rise to anisotropic transport properties in their condensed phase.

---

### 1. Introduction

Ever since the discovery of fullerenes in carbon soot, they have maintained their premier position in nanoscale sciences and technologies, because of their structural diversity arising from multiple possible arrangements of 12 pentagons and appropriate number of hexagons in hollow-cage topological networks.<sup>1-3)</sup> As in the case of other nanocarbon materials comprising  $sp^2$  C atoms, owing to the strong correlation between the  $\pi$  electron network topology and electronic structure, their detailed electronic structure strongly depends on not only fullerene cage size but also the covalent network topology. For example, the electronic structures of the 24 isomers of C<sub>84</sub> are completely different from each other, reflecting their covalent network topology, even though each isomer has the same cage size.<sup>4,5)</sup> Furthermore, their hollow-cage structures of nanometer diameter causes moderate chemical reactivity on them, which make fullerenes a starting materials for various derivatives by attaching atoms<sup>6-9)</sup> or functional groups.<sup>10-17)</sup> Depending on the modification of the  $\pi$  topology by chemical attachments, the derivatives exhibit further variation in their electronic structures not found in pristine fullerenes.

---

\*E-mail: sfurutani@comas.frsc.tsukuba.ac.jp

†E-mail: sokada@comas.frsc.tsukuba.ac.jp

Besides the versatile electronic structure of fullerenes, they have common characteristics in their  $\pi$  electronic states. It has been pointed out that the  $\pi$  electronic structures of fullerenes can be characterized as a spherical harmonic  $Y_{lm}(\theta, \phi)$ : The electronic states associated with  $\pi$  electrons tend to bunch up or degenerate, reflecting their approximately spherical distribution in the fullerene cage. Thus, the  $\pi$  electron states are regarded as an electron system confined to the spherical shell with a nanometer scale diameter.<sup>18)</sup> In addition, fullerenes and their derivatives commonly possess a deep lowest unoccupied (LU) state compared with other carbon nanomaterials and hydrocarbon molecules, owing to the twelve pentagonal rings embedded in their cages.<sup>19)</sup> Thus, fullerene and their derivatives can act as electron acceptors for electrochemical and photovoltaic applications for flexible devices. For organic thin-film photovoltaic devices, chemically decorated fullerenes act as an electron acceptor by forming the hybrid structures with appropriate donor molecules. These devices can show high open voltages owing to the deep LU state of fullerene.<sup>20–25)</sup> To further improve the power conversion efficiency, it is mandatory to give insight into the physical microscopic properties of the condensed phases of fullerene derivatives and the nanoscale structures at the bulk heterointerfaces with donor molecules.<sup>26)</sup>

In this work, we aim to clarify the electronic properties of one-dimensional chains of chemically decorated fullerenes to clarify the fundamentals of their condensed phases using the density functional theory (DFT). We considered [6,6]-phenyl- $C_{61}$ -butyric acid methyl ester (PCBM) as acceptor molecules in organic thin-film solar cells. Our calculations indicated that the binding energy and electronic structures of one-dimensional PCBM are sensitive to the mutual molecular arrangement.

## 2. Methods and Models

All theoretical calculations were conducted using DFT<sup>27,28)</sup> implemented in the STATE package.<sup>29)</sup> To express the exchange correlation potential among the interacting electrons, local density approximation (LDA) was applied with the Perdew-Wang functional form fitting to the quantum Monte Carlo results on a homogeneous electron gas,<sup>30,31)</sup> because LDA can qualitatively describe the weak interactions between graphitic  $sp^2$  C materials. We used an ultrasoft pseudopotential to describe the interactions between the valence electrons and the ions generated by the Vanderbilt scheme.<sup>32)</sup> The valence wave functions and deficit charge density were expanded by a plane-wave basis set with cutoff energies of 25 and 225 Ry, respectively. Brillouin zone integration was carried out using equidistant 21- $k$  meshes. Structural optimization was performed for both internal atomic coordinates and lattice parameters

until the remaining force acting on each atom was less than 5 mRy/Å.

To investigate the energetics and electronic structures of condensed structures of PCBM, we consider the structural model in which the PCBM form one-dimensional molecular chains for clarifying the intermolecular interactions and electronic structure under various molecular conformations, which are characterized by the intermolecular spacing  $d$  and molecular orientations of  $\theta$  and  $\phi$  as shown in Fig. 1. Since the functional moiety may mainly affect the intermolecular spacing of PCBM chains, we focus on the rotations of  $\theta$  and  $\phi$  for simplicity.

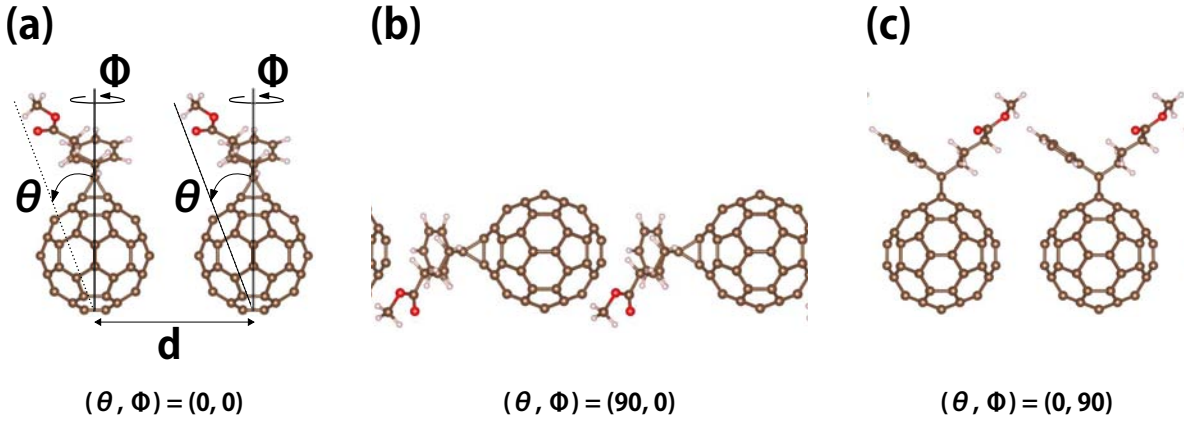


**Fig. 1.** PCBM chains with the molecular orientations  $(\theta, \phi)$  of (a)  $(0^\circ, 0^\circ)$ , (b)  $(90^\circ, 0^\circ)$ , and (c)  $(0^\circ, 90^\circ)$ .

### 3. Results and discussion

**Table I.** Binding energy and optimum lattice constant of PCBM chains with various molecular orientations.

$(\theta, \phi)$ (deg)	(0, 0)	(30, 0)	(60, 0)	(90, 0)	(0, 30)	(0, 60)	(0, 90)
Lattice constant (Å)	10.21	9.98	14.97	13.27	9.96	9.92	10.11
Binding energy (eV)	0.09	0.24	0.11	0.30	0.13	0.12	0.15

Figure 2 shows the binding energy of PCBM chains with various molecular orientations as a function of the intermolecular spacing  $d$ . The optimum spacing and binding energy of the PCBM chains are also summarized in Table I. The binding energy and optimum spacing strongly depend on the mutual molecular orientations with respect to their chain direction. The binding energy and optimum spacing are sensitive to the molecular orientation angle  $\theta$ , which corresponds to the tiling angle with respect to the molecular chain, while they are insensitive to the molecular orientation angle  $\phi$ , because of their turnip molecular shape. The

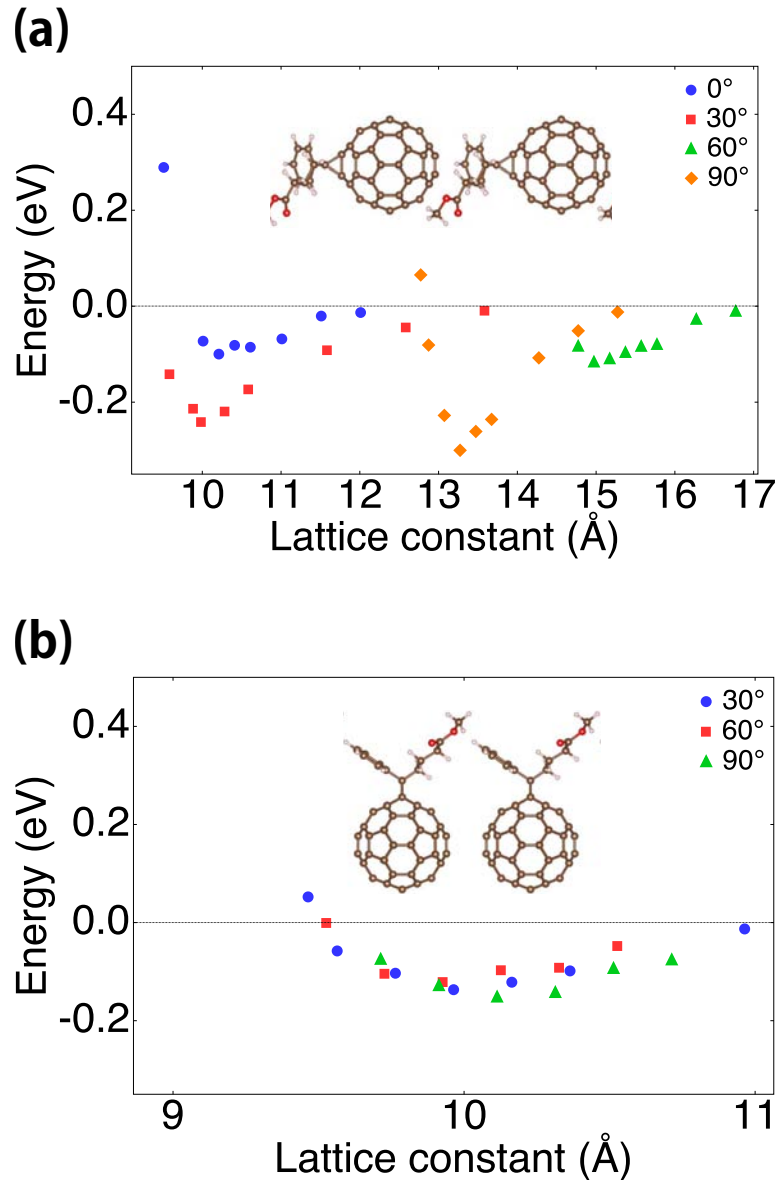


**Fig. 2.** Binding energy of one-dimensional PCBM chains as a function of intermolecular spacing under various molecular orientations of (a)  $\theta$  and (b)  $\phi$ .

optimum spacing is in the range from 9.9 to 15.0 Å, in which the binding energies range from 0.09 to 0.30 eV/mol for  $\theta$  rotation. PCBM is arranged in the head-to-tail stacking with a large spacing of 13.3 Å for their most stable chain structure, while the PCBM chains with the side-to-side molecular conformations ( $\theta = 0^\circ$  for all  $\phi$ ) with the small intermolecular spacing are the least stable structure.

Figure 3 shows the electronic band structure of PCBM chains under equilibrium intermolecular spacing for various molecular orientations of  $\theta$  and  $\phi$ . The band structure of PCBM chains strongly depends on molecular orientation, because the intermolecular spacing is sen-

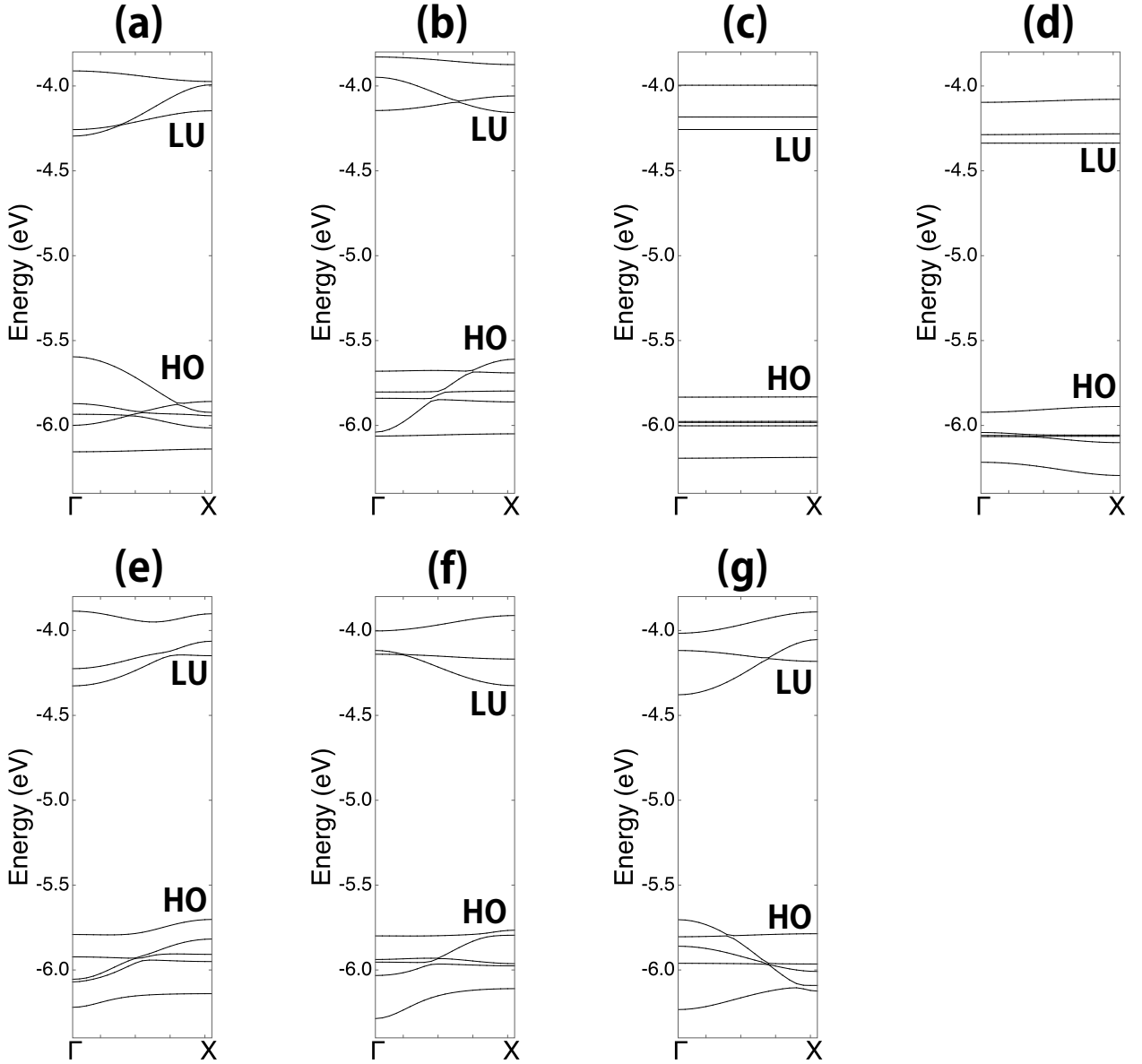


**Fig. 3.** Energy band of PCBM chain under equilibrium intermolecular spacing with molecular orientations  $(\theta, \phi)$  (a)  $(0^\circ, 0^\circ)$ , (b)  $(30^\circ, 0^\circ)$ , (c)  $(60^\circ, 0^\circ)$ , (d)  $(90^\circ, 0^\circ)$ , (e)  $(0^\circ, 30^\circ)$ , (f)  $(0^\circ, 60^\circ)$ , and (g)  $(0^\circ, 90^\circ)$ . The energies are measured from vacuum level energy. LU and HO indicate the lowest branch of the conduction band and the highest branch of the valence band, respectively.

sitive to molecular orientation, which ranges from 9.9 to 15.0 Å. For PCBM arranged in the side-to-side arrangement (the molecular orientations of  $\theta = 0^\circ$  and  $\phi = 0 \sim 90^\circ$ ), the lower branches of conduction bands possess substantial band dispersion of 0.19 eV, owing to the small intermolecular spacing of about 10 Å. On the other hand, the detailed band dispersion slightly depends on the molecular orientation. Most of the chains possess a direct band gap at the  $\Gamma$  point, except for chains with the molecular angles of  $\theta = 0^\circ$  and  $\phi = 0 \sim 30^\circ$ . In

**Table II.** Effective electron mass and band gap of various PCBM chains under the equilibrium intermolecular spacing. Direct gap (D) and indirect gap (I) of the chains are indicated in parentheses.

$(\theta, \phi)$ (deg)	(0, 0)	(30, 0)	(60, 0)	(90, 0)	(0, 30)	(0, 60)	(0, 90)
Effective mass ( $m_e$ )	0.61	0.90	634.97	95.24	0.79	0.89	0.58
Band gap (eV)	1.30 (D)	1.45 (D)	1.57 (I)	1.55 (I)	1.37 (I)	1.44 (D)	1.32 (D)

this molecular arrangement, the chain possesses an indirect band gap between the X and  $\Gamma$  points for the conduction and valence band edges, respectively. In contrast, the rotation of PCBM with respect to the angle  $\theta$  causes a substantial modulation of the band structure of the chains. The band width of the electron states around the gap is decreased by rotating the molecule with respect to the angle  $\theta$ . The chains with the molecular angles of  $\theta = 60$  and  $90^\circ$  possess narrow dispersion bands for both valence and conduction bands, owing to the large intermolecular spacing. The valence and conduction band edges are primarily distributed on the  $C_{60}$  moiety, so that the wave functions of these states hardly overlap with those in the adjacent molecules in the head-to-tail molecular arrangement  $\theta = 0^\circ$ .

The effective electron masses and energy gaps of the PCBM chains are summarized in Table II. Reflecting the band structure of the chains, the effective mass is sensitive to molecular arrangements. The smallest effective mass is  $0.58 m_e$  for the molecular orientations of  $\theta = 0^\circ$  and  $\phi = 90^\circ$ , while the largest is  $634.97 m_e$  for the orientations of  $\theta = 60^\circ$  and  $\phi = 0^\circ$ , where  $m_e$  is the bare electron mass. Note that the effective mass is insensitive to the angle  $\phi$ , because the optimum spacing is also insensitive to  $\phi$ . The fact indicates that bulk PCBM exhibits strong anisotropic transport properties, reflecting its asymmetric shape.

Finally, we discuss the correlation between the physical quantities and the intermolecular spacing to give a theoretical insight into the energetics and electronic properties of PCBM chains. Figure 4 shows the binding energy and the effective electron mass of PCBM chains as a function of equilibrium intermolecular spacing. Regarding binding energy, it does not correlate with equilibrium intermolecular spacing. Thus, PCBM is bound not only via the  $\pi$ - $\pi$  interaction between adjacent  $C_{60}$  moieties but also via the combination of  $\pi$ - $\pi$  and CH- $\pi$  interactions between the  $C_{60}$  moiety and functional groups attached to  $C_{60}$ . In contrast, for the electron effective mass, it possibly correlates with intermolecular spacing, reflecting the fact that the electronic states near the band edges are distributed on the  $C_{60}$  moiety. Thus, the electron effective masses of bulk PCBM can be estimated by investigating the intermolecular spacing along the direction corresponding to the electron transfer. This indicates that the con-

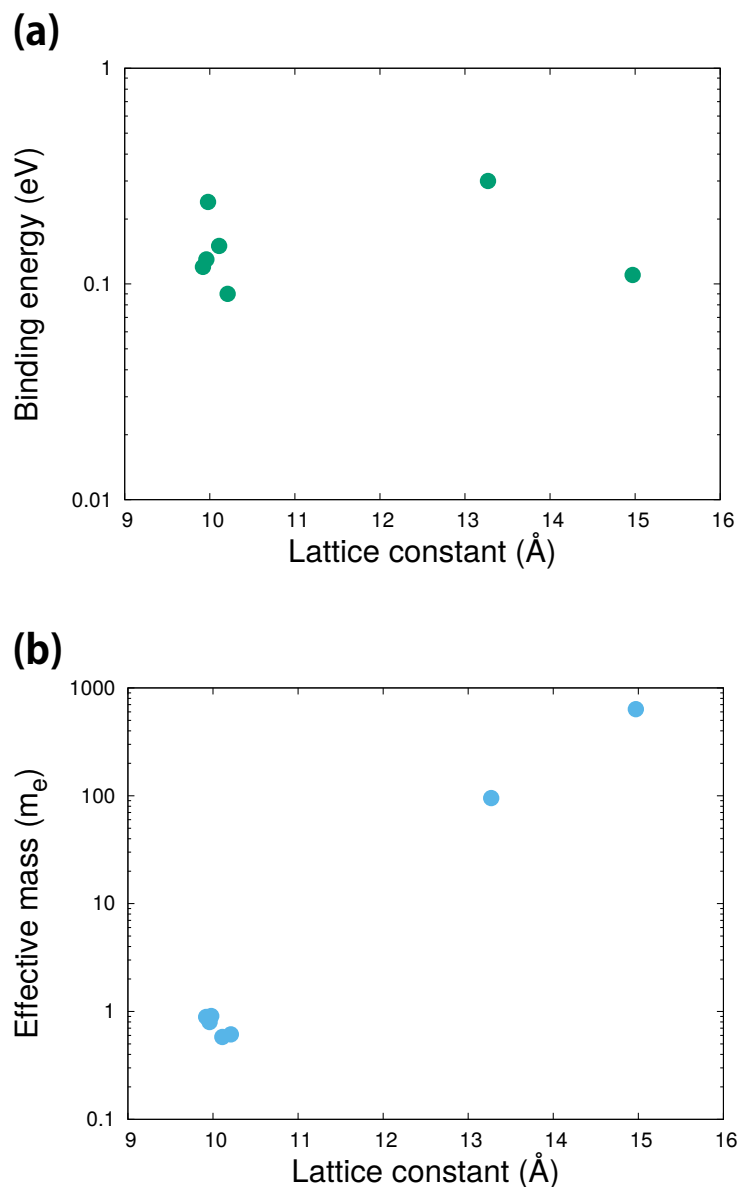


**Fig. 4.** (a) Binding energy and (b) effective electron mass of PCBM chains as a function of the equilibrium intermolecular spacing.

control of crystal orientation with respect to the electrode is mandatory for achieving remarkable carrier mobility in bulk acceptors.

#### 4. Conclusions

We studied the energetics and electronic structures of one-dimensional chain of PCBM in terms of their mutual molecular orientation using DFT with LDA. Our calculations showed that the total energy and equilibrium spacing depend on intermolecular arrangements. The calculated binding energies of PCBM range from 90 to 300 meV, depending on not only

the intermolecular spacing but also the intermolecular arrangements owing to the interaction between functional groups and  $C_{60}$ . However, the equilibrium spacing and the total energy do not correlate with each other, because of the substantial interaction between not only  $C_{60}$  moieties but also  $C_{60}$  and functional groups. We also clarified that the electronic structure of PCBM chains are also sensitive to the mutual arrangements of the PCBM chain structure. The calculated effective masses of the conduction band range from 0.58 to 634.97  $m_e$ , causing anisotropic transport properties in the condensed phase. These facts indicate that the condensed phases of PCBM may exhibit anisotropic transport properties. Therefore, it is mandatory to control the crystal orientation of bulk PCBM in OPV devices with respect to the carrier transport to further advance their power conversion efficiency.

### **Acknowledgments**

This work was supported by JST-CREST Grant Numbers JPMJCR1532 and JPMJCR1715 from the Japan Science and Technology Agency, by JSPS KAKENHI Grant Numbers JP17H01069, JP16H00898, and JP16H06331 from the Japan Society For the Promotion of Science, and by the Joint Research Program on Zero-Emission Energy Research, Institute of Advanced Energy, Kyoto University. Portions of the calculations were performed on an NEC SX-Ace at the Cybermedia Center at Osaka University and SGI ICE XA/UV at the Institute of Solid State Physics, The University of Tokyo.

**References**

- 1) M. S. Dresselhaus, G. Dresselhaus, and P. C. Eklund, *Science of Fullerenes and Carbon Nanotubes* (Academic Press, San Diego, CA, 1996).
- 2) P. W. Fowler and D. E. Manolopoulos, *An Atlas of Fullerenes* (Oxford University Press, Oxford, U.K., 1995).
- 3) D. E. Manolopoulos and P. W. Fowler, *J. Chem. Phys.* **96**, 7603 (1992).
- 4) B. L. Zhang, C. Z. Wang, and K. M. Ho, *Chem. Phys. Lett.* **193**, 225 (1992).
- 5) B. L. Zhang, C. Z. Wang, K. M. Ho, C. H. Xu, and C. T. Chan, *J. Chem. Phys.* **98**, 3095 (1993).
- 6) F. N. Tebbe, R. L. Harlow, D. B. Chase, D. L. Thorn, G. C. Campbell, J. C. Calabrese, N. Herron, R. J. Young, and E. Wasserman, *Science* **256**, 822 (1992).
- 7) S. I. Troyanov, P. A. Troshin, O. V. Boltalina, and E. Kemnitz, *Fullerenes Nanotubes Carbon Nanostruct.* **11**, 61 (2003).
- 8) J. H. Holloway, E. G. Hope, R. Taylor, G. J. Langley, A. G. Avent, T. J. Dennis, J. P. Hare, H. W. Kroto, and D. R. M. Walton, *J. Chem. Soc., Chem. Commun.* 966 (1991).
- 9) R. Taylor, J. H. Holloway, E. G. Hope, A. G. Avent, G. J. Langley, T. J. Dennis, J. P. Hare, H. W. Kroto, and D. R. M. Walton, *J. Chem. Soc., Chem. Commun.* 665 (1992).
- 10) Y. Matsuo and E. Nakamura, *Chem. Rev.* **108**, 3016 (2008).
- 11) T. Akasaka, F. Wudl, and S. Nagase, *Chemistry of Nanocarbons* (Wiley, Chichester, 2010).
- 12) M. Sawamura, K. Kawai, Y. Matsuo, K. Kanie, T. Kato, and E. Nakamura, *Nature* **419**, 702 (2002).
- 13) Y. Matsuo, A. Muramatsu, R. Hamasaki, N. Mizushita, T. Kato, and E. Nakamura, *J. Am. Chem. Soc.* **126**, 432 (2004).
- 14) S. Okada, R. Arita, Y. Matsuo, E. Nakamura, A. Oshiyama, and H. Aoki, *Chem. Phys. Lett.* **399**, 157 (2004).
- 15) E. Nakamura, K. Tahara, Y. Matsuo, and M. Sawamura, *J. Am. Chem. Soc.* **125**, 2834 (2003).
- 16) Y. Matsuo and E. Nakamura, *J. Am. Chem. Soc.* **127**, 8457 (2005).
- 17) H. Nitta, Y. Matsuo, E. Nakamura, and S. Okada, *Appl. Phys. Exp.* **6**, 045102 (2013).
- 18) J. Sorimachi and S. Okada, *Chem. Phys. Lett.* **659**, 1 (2016).
- 19) S. Saito, S. Okada, S.-I. Sawada, and N. Hamada, *Phys. Rev. Lett.* **75**, 685 (1995).
- 20) M. C. Scharber, D. Muhlbacher, M. Koppe, P. Denk, C. Waldauf, A. J. Heeger, and C. J.

- Brabec, *Adv. Mater.* **18**, 789 (2006).
- 21) F. B. Kooistra, J. Knol, F. Kastenberg, L. M. Popescu, W. J. H. Verhees, J. M. Kroon, and J. C. Hummelen, *Org. Lett.* **9**, 551 (2007).
  - 22) Y. Matsuo, Y. Sato, T. Niinomi, I. Soga, H. Tanaka, and E. Nakamura, *J. Am. Chem. Soc.* **131**, 44 (2009).
  - 23) Y. Matsuo, *Chem. Lett.* **41**, 754 (2012).
  - 24) A. Sanchez-Diaz, M. Izquierdo, S. Filippone, N. Martin, and E. Palomares, *Adv. Funct. Mater.* **20**, 2695 (2010).
  - 25) G. Garcia-Belmonte, P. P. Boix, J. Bisquert, M. Lenes, H. J. Bolink, A. La Rosa, S. Filippone, and N. Martin, *J. Phys. Chem. Lett.* **1**, 2566 (2010).
  - 26) S. Furutani and S. Okada, *Appl. Phys. Express* **9**, 115103 (2016).
  - 27) P. Hohenberg and W. Kohn, *Phys. Rev.* **136**, B864 (1964).
  - 28) W. Kohn and L. J. Sham, *Phys. Rev.* **140**, A1133 (1965).
  - 29) Y. Morikawa, K. Iwata, and K. Terakura, *Appl. Surf. Sci.* **169-170**, 11 (2001).
  - 30) J. P. Perdew and Y. Wang, *Phys. Rev. B* **45**, 13244 (1992).
  - 31) D. M. Ceperley and B. J. Alder, *Phys. Rev. Lett.* **45**, 566 (1980).
  - 32) D. Vanderbilt, *Phys. Rev. B* **41**, 7892 (1990).